

## In Situ Measurements of the Cement Hydration Profile during the Induction Period

*J.S. Schweitzer<sup>1</sup>, R.A. Livingston<sup>2</sup>, C. Rolfs<sup>3</sup>, H.-W. Becker<sup>3</sup>, S. Kubsky<sup>4</sup>, T. Spillane<sup>1</sup>, M. Castellote<sup>5</sup> and P. G. de Viedma<sup>5</sup>*

*<sup>1</sup>University of Connecticut, Storrs, CT, USA; <sup>2</sup>Federal Highway Administration, McLean, VA, USA; <sup>3</sup>Ruhr-Universität Bochum, Bochum, Germany; <sup>4</sup>Synchrotron SOLEIL, Saint-Aubin, Gif-sur-Yvette CEDEX, France; <sup>5</sup>Institute of Construction Science "Eduardo Torroja" (CSIC), Madrid, Spain*

### ABSTRACT

A better understanding of the mechanisms and kinetics of cement hydration during the induction period is critical to improved concrete technology. During the induction period a characteristic pattern of reaction layers develops at and just below the surface of the cement grain. This hydration profile can be studied nondestructively with ion beams using the  $^{15}\text{N}(p,\alpha,\gamma)^{12}\text{C}$  reaction to measure the distribution of hydrogen with depth with a spatial resolution of a few nanometers. Time-resolved measurement of the hydration profile is achieved by stopping the chemical reactions at specific times. The mechanism controlling the induction period of tricalcium silicate is a semi-permeable layer on the grain surface. The diffusion of the hydrogen cannot be represented by a simple Fickian profile, indicating that multiple diffusion and reaction processes are occurring. The hydration profiles for calcium aluminate phases are significantly different. The effects of additives on the chemical reactions are now being studied.

### 1. INTRODUCTION

The induction period is a critical stage in the cement hydration process. However a complete scientific understanding of the process has not yet been achieved. It has been established that factors such as temperature and certain types of chemicals can modify the induction time, but several competing physico-chemical models have been proposed for the mechanism that determines it [1, 2].

It is inferred from mass balance considerations based on the amount of reaction products during this period that a layer of only a few tens of nanometers on the surface of the cement grains must be involved[1]. The surface layer has been examined by several instrumental techniques [3-8], but these have yielded mostly qualitative results. We have applied a

complementary technique, nuclear resonant reaction analysis (NRRA), that provides in-situ measurements of the analytical hydrogen concentration as a function of depth with a spatial resolution of a few nanometers[9].

There are a number of nuclear resonance reactions that can be used for hydrogen detection[10]. The specific NRRA method used here is based on the ER = 6.400 MeV resonance in the  ${}^1\text{H}({}^{15}\text{N}, \alpha, \gamma){}^{12}\text{C}$  reaction. This requires a beam of nitrogen ions with very precisely regulated energies. This work is being done at the 4 MeV Dynamitron tandem accelerator at the Ruhr-Universität Bochum [10] in Bochum, Germany. This facility uses a radio-frequency system, rather than a mechanical pelletron or belt, to generate the accelerating voltage with very low ripple and good energy resolution. Moreover, careful analysis and correction of all steps from production of the beam in the ion source through acceleration and transport onto the target has been carried out to minimize the variance in the beam energy [11, 12]. This degree of precision combined with the high stopping cross section for  ${}^{15}\text{N}$  beams in cementitious materials provides an H-detection sensitivity of about 10 ppm and a H-depth resolution of a few nm at the surface. This has enabled the investigation in detail of the effect of temperature and other factors on the induction period[13-15].

## 2. EXPERIMENTAL APPROACH

The basic experimental procedure has been described elsewhere[9]. A major difference between this method and others used for studying cement chemistry, such as calorimetry, is that the material under investigation is not in powdered form, but is rather a solid object, in order to present a well-defined smooth surface to the ion beam. Cementitious phases such as tricalcium silicate ( $\text{C}_3\text{S}$ ) and tricalcium aluminate ( $\text{C}_3\text{A}$ ) were molded into cylindrical pellets of 12.7 mm diameter and then fused. A typical experimental run for determining the induction time for a particular condition consists of 8-12 samples, not including control samples. They are hydrated in a common bath of solution of specified composition and temperature, and individual samples are then removed at specific times for analysis. The samples are stored and handled under inert atmosphere both before and after the chemical reaction. Reacted samples are kept in a vacuum system until analysis. Each sample thus represents a single point in the material's hydration time history.

To probe the sample's H depth profile, the beam energy is increased stepwise starting just below the resonance energy of 6.400 MeV. At each energy step, a  $\gamma$ -ray spectrum is acquired, typically 10,000 cts per minute. The beam energy is increased in 10 keV steps to 7 MeV to resolve thin surface layers, and then in coarser steps (100-500 keV) as the profile

typically changes more slowly in this region. The maximum beam energy was limited to 12 MeV to avoid interference from the next higher energy resonance. Owing to the strong isolated resonance in the H capture cross section, the reaction only occurs when the  $^{15}\text{N}$  ion energy is at the resonance energy. If its energy is greater than the resonance, no reactions occur until it loses enough energy by scattering to get down to the resonance energy. Thus for each beam energy step, the  $^{15}\text{N}$  ion will reach the resonance energy at a particular depth in the sample, and the hydrogen concentration at that depth is measured. By plotting the hydrogen signal as a function of incident beam energy it is possible to visualize the hydrogen depth profile.

An example of such a profile is shown in Figure 1. This is for a  $\text{C}_3\text{S}$  sample during the induction period. It shows the typical Gaussian peak associated with a surface layer, on the left edge of the figure, followed by a diffusion-type region extending into the sample. The NRA coordinates of beam energy and counts per charge have been converted to depth and H concentrations on the upper horizontal and right vertical axes respectively.

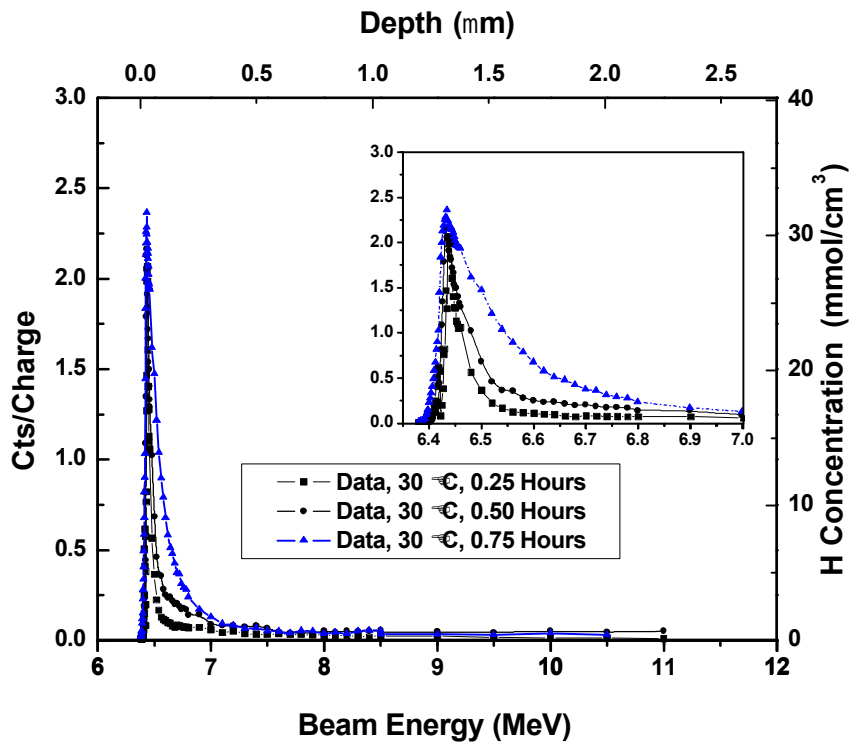


Figure 1: Progression of hydrogen concentrations with depth and time during the early induction period for triclinic  $\text{C}_3\text{S}$  hydrated at  $30\text{ }^\circ\text{C}$

The Gaussian peak is interpreted as a semi-permeable surface layer. This allows the calcium ions to migrate into the solution in exchange for water ions, but the larger silicate ions are trapped below the surface in the form of a silica gel. A schematic of the various layers is shown in Fig. 2. The gel has a larger volume than the  $C_3S$ , and as it grows it exerts stresses on the surface layer. Eventually the stress exceeds the strength of the layer, and it ruptures, releasing the trapped silica into the pore solution, where it reacts with the calcium ions to form the C-S-H gel. This breakdown of the surface layer marks the end of the induction period.

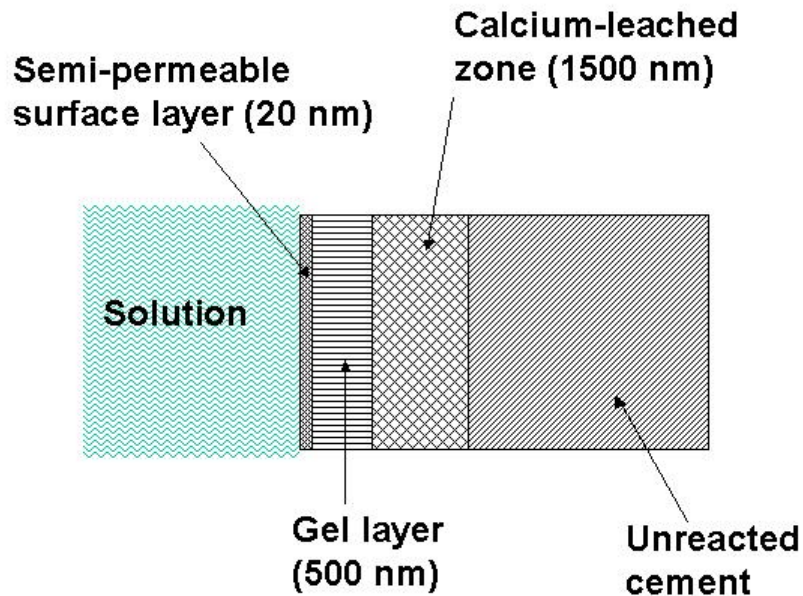


Figure 2: Reaction zones in hydrating  $C_3S$  during the induction period.

Profiles for three different times are plotted Fig. 1 to illustrate how the diffusion region grows while the Gaussian peak remains fixed. The end of the induction period is characterized by the breakdown of the surface layer. This is easily recognized in the profiles by the absence of the Gaussian peak and a change in the shape of the diffusion region curve. We are able to determine the time at the end of the induction period to a relative precision generally better than 5%

In Fig 3a a typical hydrogen profile shortly after the start of the induction period is presented. Figure 3b shows the hydrogen profile at approximately the time of breakdown. It can be seen that the diffusion-gradient region is much larger, and the hydrogen concentration near the surface exceeds that of the semi-permeable layer.

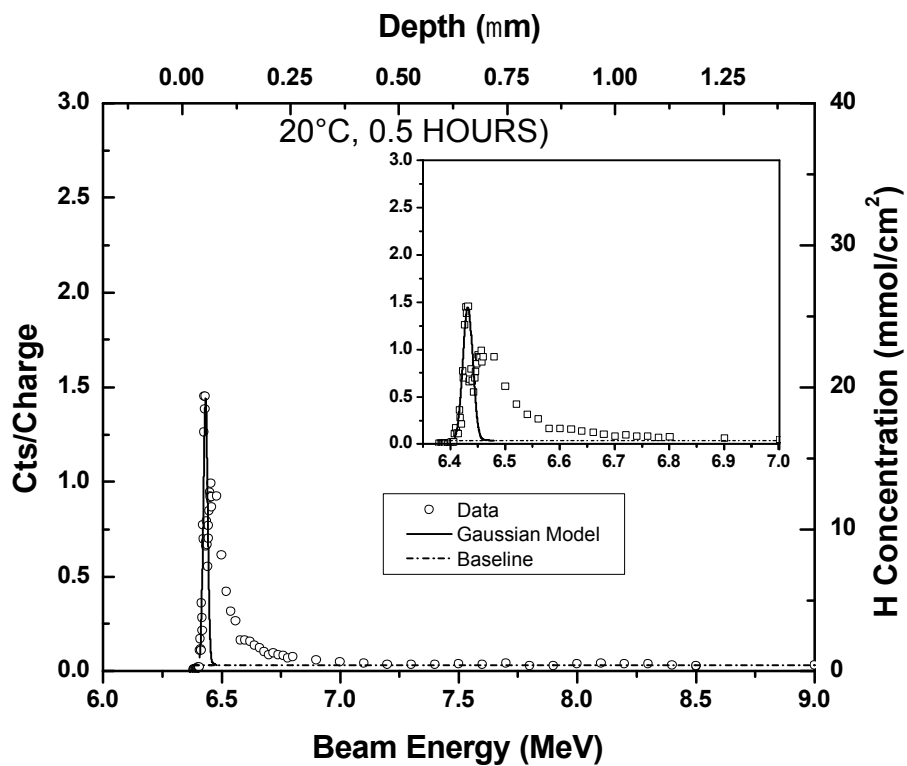


Figure 3a: Hydrogen depth profile for triclinic  $C_3S$  at 0.5 hrs and 20 °C

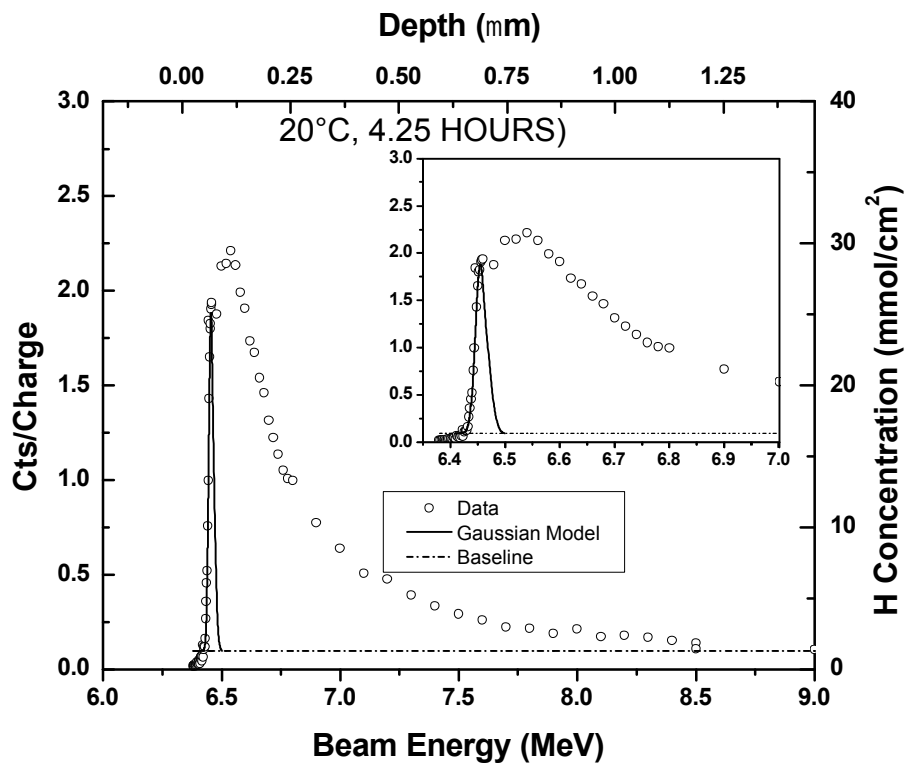


Figure 3b: Hydrogen depth profile for triclinic  $C_3S$  at 4.25 hrs and 20 °C

This proposed mechanism for the end of the induction period differs from the one prevailing in the literature which states that the mechanism is the rapid nucleation and precipitation of CH after achieving and maintaining supersaturation for a certain period of time [2]. That process cannot be happening in this set of experiments because the solution is kept in equilibrium with solid CH at all times. Moreover, in the original paper proposing the CH supersaturation mechanism, Young et al. point out several issues[16]. One is the difficulty of determining the start of nucleation of the CH crystals. Another is that the supersaturation appears to increase after onset of nucleation. Also, the end of the induction period is determined by calorimetry, which can lag behind the actual reaction rate. In a very recent set of experiments, Grant et al. found that the rapid drop in  $\text{Ca}^{2+}$  as measured by conductivity, coincided with the peak reaction rate and not with the end of the induction period[17]. Young et al. called for "...improved methods of analysis clearly need to be developed for future work".

NRRA provides such an improved method that can help resolve these issues by permitting direct visualization of the surface layers. During the induction period the  $\text{Ca}^{2+}$  concentration can slowly increase, but there is no silicate ion available to form C-S-H. After the breakdown of the semi permeable layer, the  $\text{C}_3\text{S}$  can dissolve more rapidly and congruently, thus the  $\text{Ca}^{2+}$  concentration can continue to increase. The simultaneous release of the silicate ions can initiate the formation of C-S-H which removes the  $\text{Ca}^{2+}$  rapidly from the solution. It should be noted that this mechanism of a surface layer permeable to Ca and water but impermeable to silicate ion has been proposed by others in the past such as Jennings and Pratt [18] and Dent Glasser [19]. However, prior to the introduction of NRRA it was not possible to actually determine the actual pattern of these layers.

In future research with NRRA, one proposed set of experiments would involve hydration of the  $\text{C}_3\text{S}$  pellets starting with distilled water, instead of saturated lime water, in order to replicate the experimental conditions of Young et al. However, this would require significant redesign of the hydration apparatus in order to provide the correct water/cement ratio. This issue of pellets vs powders was encountered by Menetrier et al [6] in observing the surface layers using ESCA and SIM. However, because of the limited depth penetration of ESCA( ~2 nm), their research concerned the development of the surface layer at the start of the induction period. In contrast, the NRRA investigations concern the end of the induction period. The induction times measured on  $\text{C}_3\text{S}$  pellets using NRRA are in very good agreement with the times inferred from other types of measurements on powders such as quasi-elastic neutron scattering [20].

### 3. EFFECT OF CEMENTITIOUS PHASE COMPOSITION

One set of experiments with NRRA investigated the development of the hydration profiles for different cementitious phases hydrated under fixed solution conditions, i.e. a pH 12.4 solution saturated with respect to CH. Both tricalcium and dicalcium silicate were studied as well as tricalcium aluminate. A series of glasses simulating fly ash glasses was also investigated, but this research is presented in another paper in these proceedings[21].

#### 3.1 Tricalcium silicate

This actually occurs in several polymorphs[1]. The pure phase is triclinic, but the phase typically found in Portland cement is monoclinic, due to the incorporation of impurities such as aluminum or magnesium. To minimize any confounding effects of these impurities, the first set of experiments was performed on triclinic  $C_3S$ . Typical hydration profiles at 30°C are shown above in Fig. 1. The first set of experiments concerned the effect of temperature on the kinetics of the induction period. Isothermal hydration series were conducted at three different temperatures: 10, 20 or 30° C.

The breakdown times were determined and are plotted in Fig. 4 as a semi-log graph vs inverse temperature. The result agreed very well with an Arrhenius-type behavior with an activation energy of  $69 \pm 4$  kJ/mol.

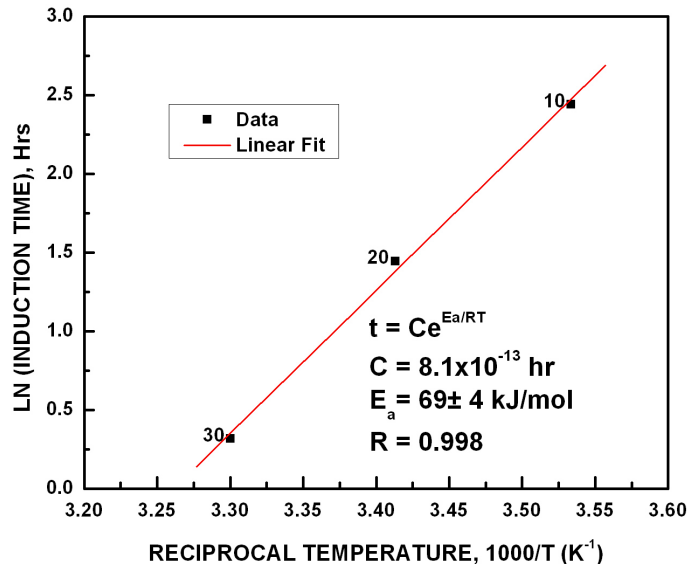


Figure 4: Arrhenius plot of induction times for  $C_3S$

A subsequent set of experiments compared the hydration profile development of the monoclinic  $C_3S$  polymorph against that of the triclinic. Figure 4 presents the results at 1.5 hrs. The triclinic phase has already reached the end of the induction period as can be seen in the jagged profile at the left where the Gaussian peak would normally be during the induction period. The monoclinic phase is still in the induction period.

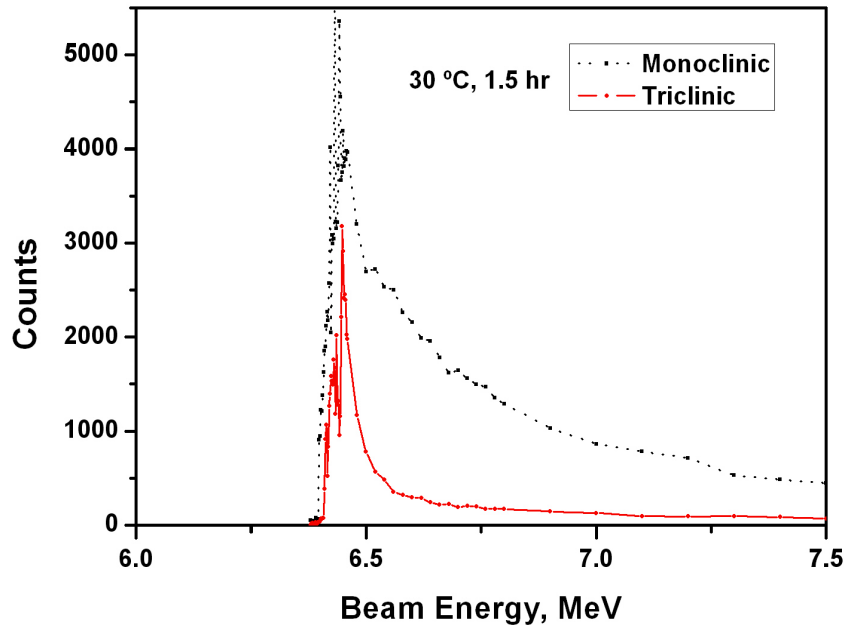


Figure 5: Comparison of triclinic vs. monoclinic  $C_3S$  Hydration profiles at 1.5 hrs.

### 3.2 Dicalcium silicate

A third set of experiments compared the hydration of triclinic  $C_3S$  against another Portland cement constituent, dicalcium silicate ( $C_2S$ ). As shown in Fig. 5, both phases develop a surface layer, but the diffusion region in the  $C_2S$  at 1.25 hrs at 30° C is much less developed than in the  $C_3S$ . This is consistent with the well-established fact that the former is much less reactive than the latter. Examination of the other profiles in the  $C_2S$  time series indicates that it doesn't reach the end of the induction period until about 7 hrs at 30° C.



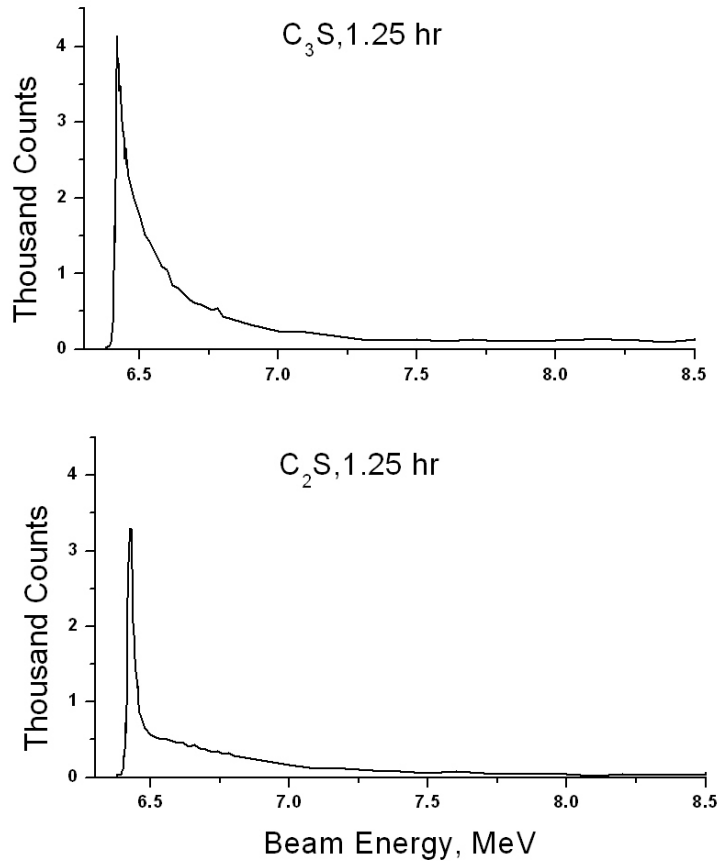


Figure 6: Comparison of hydration profiles of triclinic C<sub>3</sub>S vs. C<sub>2</sub>S at 1.25 hrs.

### 3.3 Tricalcium aluminate

Finally, the most recent experiments have investigated the hydration of one of the aluminate phases in Portland cement, tricalcium aluminate (C<sub>3</sub>A). This is known to react very rapidly and can cause false setting of the concrete [1]. To avoid this, gypsum is added to the cement. This provides sulfate ions that react with the C<sub>3</sub>A to provide ettringite which is thought to slow down set. In fact, Billingham and Coveney[22] have proposed that this reaction controls the overall setting process. However, as discussed above, the induction period is determined by the C<sub>3</sub>S hydration in the absence of C<sub>3</sub>A and gypsum. In any case, for these hydration experiments, it was decided to try to slow the reaction by maintaining the solution at 10° C and dissolving some calcium sulfate in the solution. Also, the samples were removed from the solution at very short time intervals of 5 or 10 minutes.

The results are plotted in Fig. 6. They are significantly different in shape from the profiles typically seen in hydrating calcium silicates. Nevertheless, except for the blank sample, all of them show very similar characteristic features. There is a very well defined leading edge, representing the hydrated surface of the specimen. This is also nearly vertical and occurs at the same energy for all hydration times. Next there is a step, which is not evident at the early ages, but tends to develop with time. There may be some minor features in this region, such as a small peak where the step meets the leading edge. Third, there is the main peak that occurs at around 6.5 MeV. With time, this tends to shrink and to move toward slightly higher energies. Finally, there is a nonlinear gradient tailing off at higher energies.

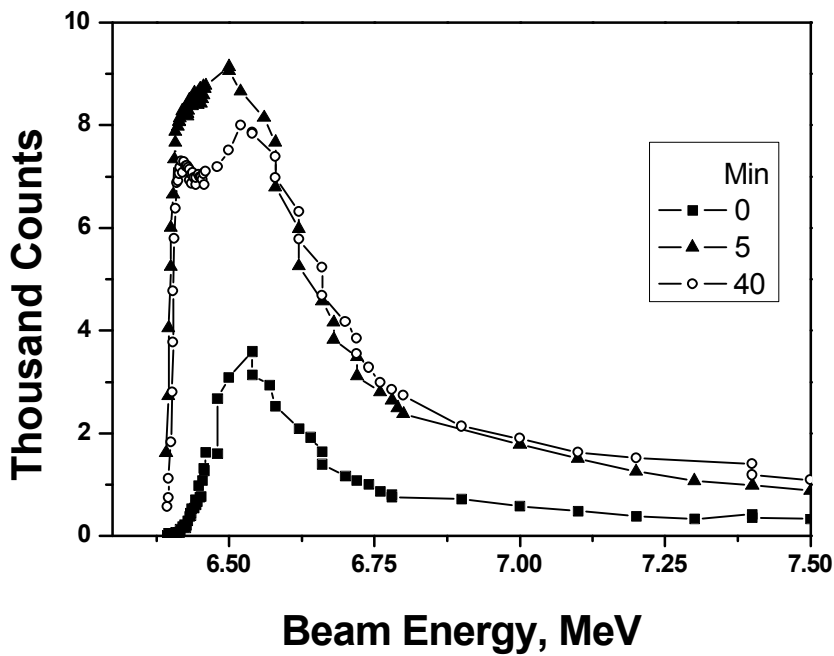


Figure 7: Hydration profiles for C<sub>3</sub>A at various times.

A preliminary interpretation of these features is that the vertical leading edge and step represent a zone of crystalline material. Given the nominal solution chemistry this would be a mixture of CH and ettringite. The jaggedness of the step may be due to NRRA interactions with individual crystals projecting from the surface. The main peak behind it could be due to a disordered aluminate gel containing additional water in the gel pores. Finally, the gradient represents a zone of leaching and exchange between water and calcium.

In terms of kinetics, the curves appear to be remarkably stationary. As Fig. 5 shows, the only apparent changes with time appear to be the development of the step and the reduced height of the main peak. Unlike the calcium silicate phases, the gradient region does not grow deeper into the substrate. In other words, in the first five minutes, the diffusion of water reaches a critical depth and then stops. A possible explanation for this is that initially water diffuses into the  $C_3A$  and exchanges with calcium ions. These in turn react at the surface to form some crystalline layer that tends to act as a diffusion barrier. Sometime before 5 minutes, this barrier develops enough to completely stop further diffusion. An explanation for the development of the step over time may be that the material in the peak region is initially some katoite (calcium aluminate hydrate) phase. Over time this converts to ettringite as sulfate ions diffuse in from the surface. It is planned to examine the surface layers with X-ray diffraction to determine the exact nature of the crystalline phases.

#### 4. ACCELERATORS AND RETARDERS

As noted above, there are a number of chemicals that can accelerate or retard the hydration process [1]. They can be simple inorganic salts like calcium chloride or complex organic compounds, often involving carboxylates. For example, lignosulfonates, often used as retarders, are waste products from the wood pulp industry and consist of three-dimensional random polymers with molecular weights up to 50,000. They also contain various other organic compounds such as sugars and gluconates that also act as retarders. At present, mechanisms through which acceleration and retardation occurs are not completely understood. Some theories maintain that it involves absorption on surfaces, others that it involves effects on solubility of various chemical species.

As a preliminary step in investigating these effects some hydration experiments were carried out on  $C_3S$  pellets using either a classic accelerator, calcium chloride, or a retarder, sucrose. A comparison of the profiles is given in Fig. 7. Both samples were hydrated at  $30^\circ\text{C}$ . For the calcium chloride solution, at 1.5 hours, the surface layer has already broken down. In contrast, for the sucrose at 24 hours, the longest time interval reached in these experiments, the surface layer is still present, and the diffusion region has barely started to develop.

Current research on retarders is focused on sodium gluconate, which is a major ingredient in commercially available retarders. The initial set of experiments has shown that adding as little as 0.013% by weight of sodium gluconate to the solution significantly reduces the rate of hydration. Increasing the dosage to 0.018% slows the hydration by a factor of 2.7.

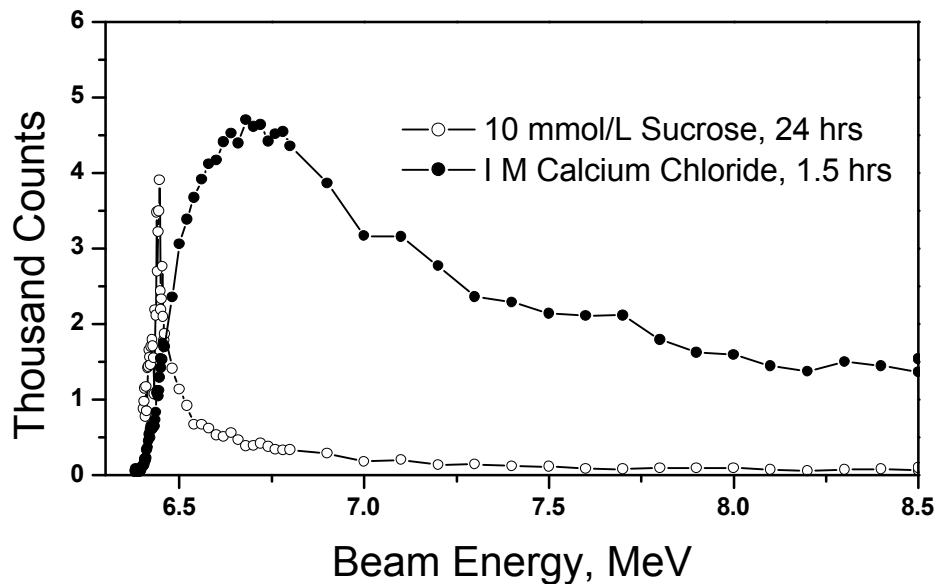


Figure 8: Comparison of sucrose and calcium chloride admixtures

## 5. SUMMARY

We have used the spatial sensitivity of the  $^1\text{H}(^{15}\text{N}, \alpha, \gamma)^{12}\text{C}$  reaction to investigate the physical and chemical processes involved in the hydration of various components of Portland cement at the nanometer scale. This has provided new insights into the mechanisms that control the setting and curing of concrete and has helped to resolve some longstanding controversies. For the calcium silicate phases, there is generally the development of a semi-permeable surface layer that controls the hydration rate of reaction during the induction period. However, there are some differences in the rates of reaction between the polymorphs of  $\text{C}_3\text{S}$  and between  $\text{C}_3\text{S}$  and  $\text{C}_2\text{S}$ . The length of the induction period shows a classic Arrhenius-type dependence on temperature.

Tricalcium aluminate shows a very different spatial pattern of hydration. There is no semi-permeable surface layer. Instead a crystalline layer develops almost immediately, and apparently halts further reaction with water.

Initial experiments with accelerators and retarders have shown that they significantly affect the development the hydration profile, either by changing the permeability of the surface layer or the diffusion coefficients in the substrate. For a commercially available retarder like sodium gluconate, the rate of hydration is strongly dependent on the dosage.

## 6. ACKNOWLEDGEMENTS

The authors are indebted to the support of the National Science Foundation under contract CMS-0600532 that made this research possible.

## 7. REFERENCES

[1] H. F. W. Taylor, Cement Chemistry, 2nd Edition, Thomas Telford, London, 1997

[2] J. F. Young, Tricalcium Silicate Hydration: A Historical Overview, in: Young, J. F. and Skalny, J. (Eds.), Materials Science of Concrete VII, The American Ceramic Society, Westerville, OH, 2005, pp. 101-118

[3] E. Henderson and J. E. Bailey, The compositional and molecular character of the calcium silicate hydrates formed in the paste hydration of  $3\text{CaOSiO}_2$ , J Mat Sci 28 (1993) 3681-3691

[4] D. Menetrier, I. Jawed, T. S. Sun and J. Skalny, ESCA and SEM Studies of Early C3S Hydration, Cem Con Res 9 (1979) 473

[5] P. Meredith, A. M. Donald and K. Luke, Pre-induction and induction hydration of tricalcium silicate: An environmental scanning electron microscope study, J Mat Sci 30 (1995) 1921-1930

[6] L. D. Mitchell, M. Prica and J. D. Birchall, Aspects of Portland cement hydration studied using atomic force microscopy, J Mat Sci 31 (1996) 4207-4212

[7] K. Scrivener, The Microstructure of Anhydrous Cement and its Effect on Hydration, in: Struble, L. J. and Brown, P. W. (Eds.) Microstructural Development During Hydration of Cement, MRS Symposium Vol. 85, Materials Research Society, 1987 pp. 39-46.

[8] D. Viehland, J.-F. Li, L.-J. Yuan and Z. Xu, Mesostructure of Calcium Silicate Hydrate (C-S-H) Gels in Portland Cement Paste: Short-Range Ordering, Nanocrystallinity, and Local Compositional Order, J Am Ceram Soc 79 (7) (1996) 1731-44

[9] R. A. Livingston, J. S. Schweitzer, C. Rolfs, H.-W. Becker and S. Kubsky, Characterization of the Induction Period in Tricalcium Silicate Hydration by Nuclear Resonance Reaction Analysis, J Mat Res 16 (3) (2001) 687-693

- [10] W. A. Lanford, Nuclear Reactions for Hydrogen Analysis, in: Tesmer, J. and Nastasi, M. (Eds.), Handbook of Modern Ion Beam Analysis Materials Research Society, Pittsburgh, 1995, pp. 193
- [11] S. Wüstenbecker, H. W. Becker, C. Rolfs, H. P. Trautvetter, K. Brand, G. E. Mitchell and J. S. Schweitzer, Technical developments for ion beams with high energy resolution, Nuc Instr Meth A 256 (1987) 9-22
- [12] L. Borucki, H. W. Becker, F. Gorris, S. Kubsky, W. H. Schulte and C. Rolfs, Hydrogen Doppler spectroscopy using  $^{15}\text{N}$  ions, Eur J Phys A5 (1999) 327-336
- [13] J. S. Schweitzer, R. A. Livingston, C. Rolfs, H.-W. Becker and S. Kubsky, Study of Cement Chemistry with Nuclear Resonant Reaction Analysis, in: in: Duggan, J. L. and Morgan, I. L. (Eds.), Applications of Accelerators in Research and Industry, Proceedings of the Sixteenth International Conference, American Institute of Physics, Denton, Texas, 2001, pp. 1077-1080
- [14] J. S. Schweitzer, R. A. Livingston, C. Rolfs, H.-W. Becker and S. Kubsky, Ion beam analysis of the hydration of tricalcium silicate, Nucl Instr Meth B 207 (1) (2003) 80-84
- [15] J. S. Schweitzer, R. A. Livingston, C. Rolfs, H.-W. Becker, S. Kubsky, T. Spillane, M. Castellote and P. Garcia De Viedma, Nanoscale studies of cement chemistry with  $^{15}\text{N}$  Resonance Reaction Analysis, Nucl Instr Meth B 241 (2005) 441-445
- [16] J. F. Young, H. S. Tong and R. L. Berger, Compositions of Solutions in Contact with Hydrating Tricalcium Silicate Pastes, J Am Ceram Soc 60 (5) (1977) 193-198
- [17] S. A. Grant, G. E. Boitnott, C. J. Korhonen and R. S. Sletten, Effect of temperature on hydration kinetics and polymerization of tricalcium silicate in stirred suspensions of CaO-saturated solutions, Cem Con Res 36 (2006) 671 - 677
- [18] H.M Jennings and P.L. Pratt, An experimental argument for the existence of a protective membrane surrounding Portland cement during the induction period, Cem Con Res 9 (1979) 501-506.
- [19] L.S. Dent Glasser, Osmotic Pressure and the Swelling of Gels, Cem Con Res 9 (1979) 515-517.

[20] S. Fitzgerald, D. Neumann, J. Rush and R. Livingston, In-situ Quasi-elastic Neutron Scattering Measurement of the Hydration of Tricalcium Silicate, Chem Mater 10 (1) (1998) 397-402

[21] W. Bumrongjaroen, R. A. Livingston, J. S. Schweitzer and I. Muller, Fly Ash Reactivity as a Glass Corrosion Problem, in: in: Beaudoin, J. (Ed.) 12th International Congress on the Chemistry of Cement, Montreal, 2007, in press

[22] J. Billingham and P. V. Coveney, Simple Chemical Clock Reactions: Application to Cement Hydration, J Chem Soc Faraday Trans 86 (6) (1993) 3021-3028